Supporting Information

Electrochemically Synthesized Fe–Mn Mesh Catalysts for Catalytic Ozonation Degradation of Phenol

Fengyin Sun[1,†], Haoyuan Gu[1,†], Jing Wang[1], Jing Xu[1,2]*, Minghui Zhu[1]*

[1] State Key Laboratory of Green Chemical Engineering and Industrial Catalysis, School of Chemical Engineering, East China University of Science and Technology, Shanghai 200237, China.

[2] University Engineering Research Center of Green Chemical New Materials, School of Chemistry and Chemical Engineering, Guangxi University, Nanning, Guangxi, 530004, China.

[†] These authors contributed equally.

*Corresponding author E-mail: xujing@ecust.edu.cn (J.X.); minghuizhu@ecust.edu.cn (M.Z.)

S1 Catalyst appearance and elemental composition

After electrochemical treatment, a non-uniform brown-yellow deposit was observed on the surface of FM, whereas the introduction of Mn generally produced a denser and more uniform deposit on the *x*-FMM surface, most clearly for 0.04FMM and 0.08FMM (Fig. S1). The elemental composition of the *x*-FMM catalysts, determined by ICP-OES, is summarized in Table S1. The balance of the mass (< 100 wt%) consists of oxygen and other light elements from the $FeO(OH)/Fe_2O_3/MnO_x$ phases identified by XRD/XPS. Notably, the Mn loading is non-monotonic with electrolyte concentration (8.51 → 14.24 → 11.28 wt% for 0.04, 0.08, and 0.12 mol L^{-1} $Mn(NO_3)_2$, respectively), consistent with the aggravated aggregation observed by SEM for 0.12FMM. The concurrent monotonic increase of Fe loading (42.62 → 63.25 → 68.11 wt%) suggests that the non-monotonic Mn content is not explained by bulk deposit detachment alone, but more likely reflects a compositional shift driven by reduced Mn-deposition efficiency at the highest electrolyte concentration. 0.04FMM was included here to illustrate this compositional trend. To keep the characterisation workload tractable, the subsequent BET, SEM, XRD, and XPS analyses focused on FM (as a Mn-free reference), 0.08FMM (highest Mn loading) and 0.12FMM (highest electrolyte concentration).

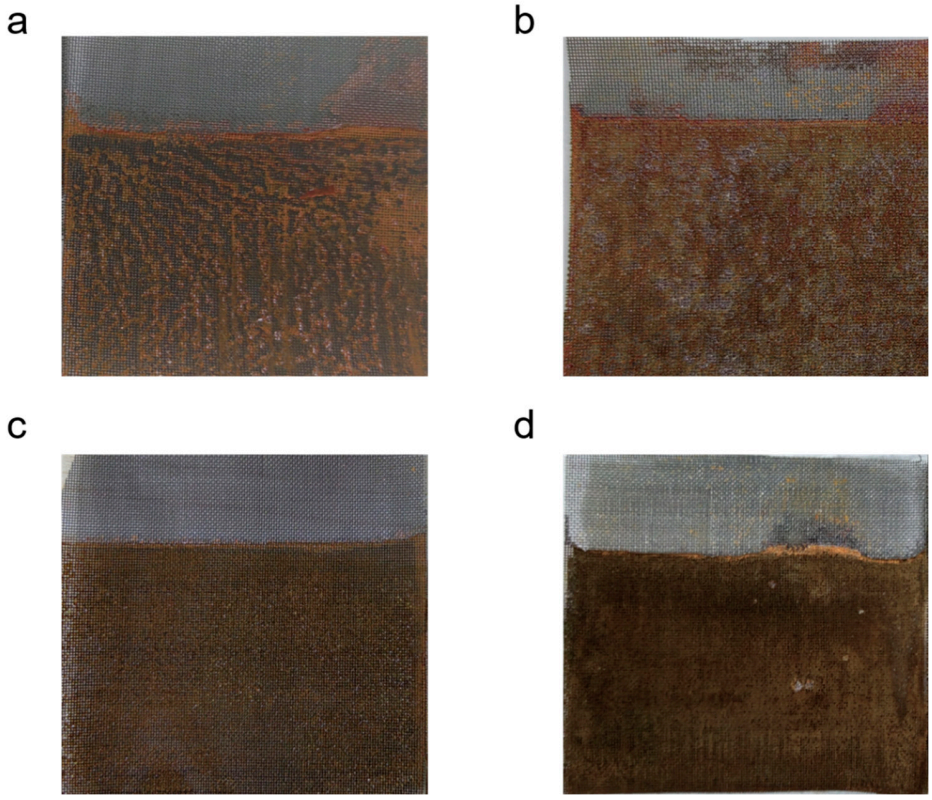


Fig. S1 Photographs of (a) FM, (b) 0.04FMM, (c) 0.08FMM, and (d) 0.12FMM after electrochemical deposition and drying at 60 °C for 2 h, photographed under ambient laboratory lighting against a white background. Each mesh sample is approximately 6 × 4 cm.

Table S1 Mn and Fe contents of *x*-FMM catalysts.

Catalysts	Content of Mn (wt.%)	Content of Fe (wt.%)
0.04FMM	8.51 ± 0.14	42.62 ± 0.25
0.08FMM	14.24 ± 0.21	63.25 ± 0.29
0.12FMM	11.28 ± 0.16	68.11 ± 0.32

S2 Adsorption control experiments

Fig. S2 and Table S2 show the phenol adsorption curves and the BET specific surface areas of FM and FMM catalysts, respectively, which are discussed together in Section 2.1 of the main text.

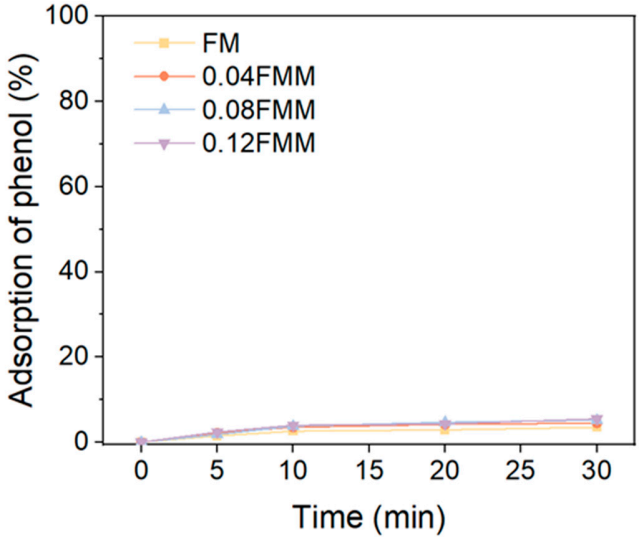


Fig. S2 Adsorption of phenol by FM and FMM catalysts.

Table S2 BET specific surface areas of FM and FMM catalysts.

Catalysts	BET surface area (m^2 g^{-1})
FM	0.6
0.08FMM	1.5
0.12FMM	2.8

S3 Optimization of electrodeposition parameters

Fig. S3 compares the phenol removal over 0.04FMM, 0.08FMM, and 0.12FMM across the full screening range. At the optimum condition (±180 mA, 9000 s, 30 s per cycle), phenol removal decreases in the order 0.08FMM (87.8%) > 0.04FMM (84.1%) > 0.12FMM (82.5%). Both scans show volcano-type dependences, with performance dropping by 4–13 percentage points once either parameter departs from the optimum. 0.08FMM is the best-performing sample across every screening point except at 12000 s, where the three catalysts converge within 5 pp.

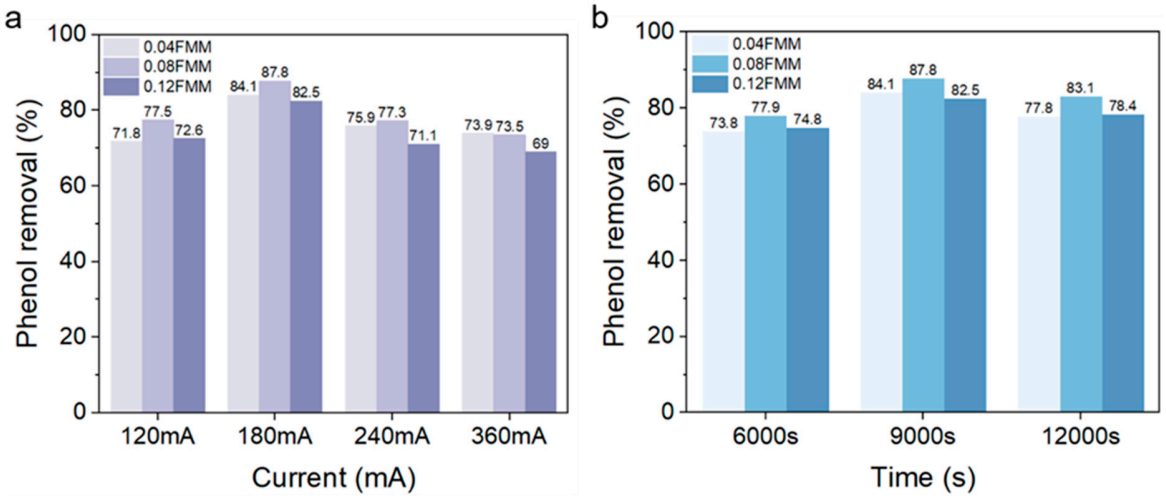


Fig. S3 Effects of (a) current and (b) total time during electrodeposition on the catalytic ozonation performance of FMM catalysts for phenol removal. In (a) the total deposition time was fixed at 9000 s; in (b) the current was fixed at ±180 mA; in both panels each cycle was 30 s. Catalytic test conditions: $[phenol]_0$ = 300 mg L^{-1}, O_3 feed rate = 6 mg min^{-1} (0.2 L min^{-1} pure O_2 carrying 30 mg L^{-1} O_3), catalyst loading ~1 g, 25 °C, 30 min reaction time.

S4 Effect of initial pH on phenol removal

It is well known that the efficiency of ozonation differs substantially under acidic and alkaline conditions [30], so the initial solution pH is an important factor in catalytic ozonation [31]. Fig. S4 shows the phenol-removal efficiency at initial pH of 4, 7, and 11. In the absence of a catalyst, phenol removal rose monotonically with pH (32%, 48%, and 59% at pH 4, 7, and 11, respectively), consistent with the known base-catalysed self-decomposition of ozone that enhances HO· formation in alkaline solution. In contrast, 0.08FMM gave 78%, 85%, and 82% phenol removal at the same three pH values, varying by only ~7 percentage points across the 4–11 range. The mechanistic origin of this pH insensitivity is discussed in Section 2.1 of the main text.

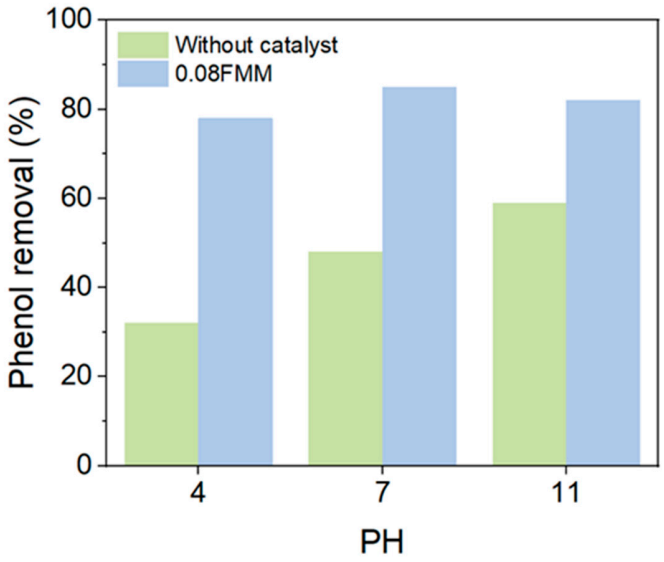


Fig. S4 Phenol removal at initial pH of 4, 7, and 11 over 0.08FMM and in the absence of a catalyst. Initial pH was adjusted with 0.1 mol L^{-1} HCl or NaOH; no buffer was used, so the pH may drift during the 30 min reaction. Other catalytic test conditions as in Fig. S3.

S5 Long-term catalytic stability and metal leaching

The long-term catalytic performance of 0.08FMM was evaluated under the optimized electrodeposition and catalytic conditions for 20 h of continuous operation. Phenol removal and dissolved Fe and Mn concentrations were monitored periodically; Fe and Mn concentrations were determined by ICP-OES. Other catalytic test conditions were the same as those given for Fig. S3. Phenol removal decreased from approximately 87.7% at the beginning of the test to ~82% during the initial 2 h and then remained near 79–80% through 20 h. Fe leaching decreased from ~18.6 μg L^{-1} initially to ~4–5 μg L^{-1} at 20 h, while Mn leaching decreased from ~5–6 to ~1–2 μg L^{-1}. The initial activity decrease followed by a plateau, together with the declining Fe and Mn concentrations, is consistent with an initial conditioning process involving removal of weakly bound surface species followed by retention of a more strongly anchored catalytic layer.

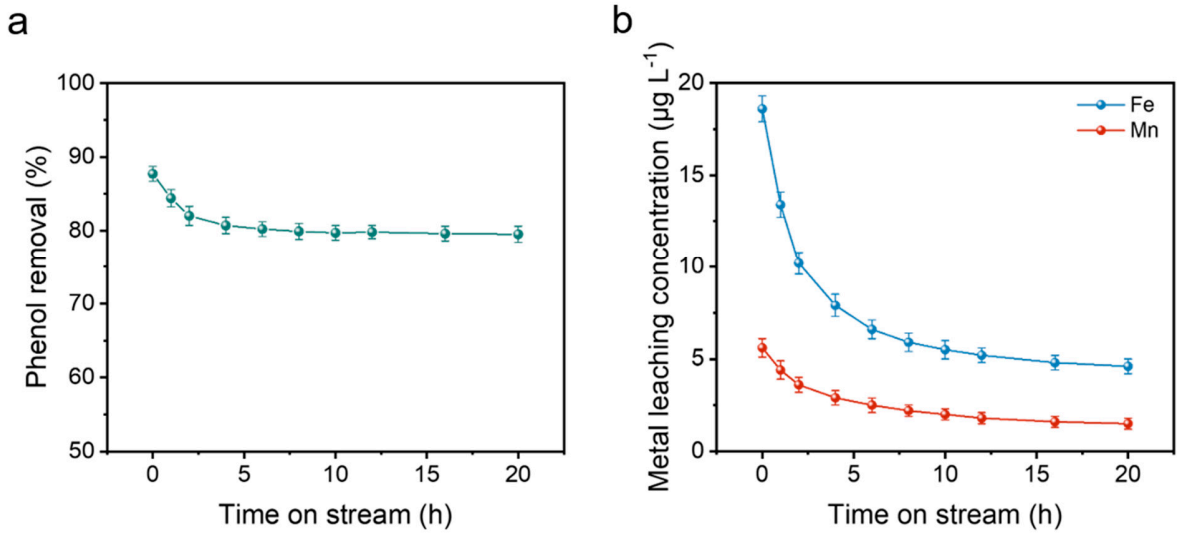


Fig. S5 (a) Phenol removal and (b) Fe and Mn leaching concentrations during 20 h continuous operation of 0.08FMM under optimized conditions.

S6 ATR-FTIR characterization before and after reaction

ATR-FTIR spectra of FM and 0.08FMM were collected before and after catalytic ozonation using attenuated-total-reflectance mode at room temperature. Fresh and post-reaction samples were subjected to the same drying protocol before analysis. A fresh background was collected before each measurement; spectra were background-corrected and normalized to the comparatively stable metal–oxygen vibration region (450–750 cm^{-1}) before comparison. The integrated broad O–H envelope at 3000–3700 cm^{-1} was used for semi-quantitative comparison. For 0.08FMM, the integrated O–H envelope decreased by approximately 28% after reaction, compared with an approximately 8% decrease for FM. The H–O–H bending region near 1630 cm^{-1} showed a smaller change, while the main metal–oxygen bands in the 450–750 cm^{-1} region remained comparatively unchanged. Because adsorbed molecular water can also contribute to the broad O–H stretching envelope, the FTIR result is interpreted together with the O 1s XPS, Na_3PO_4-blocking, and EPR results rather than as a species-exclusive assignment. All spectra were acquired under identical instrumental settings for direct comparison among samples.

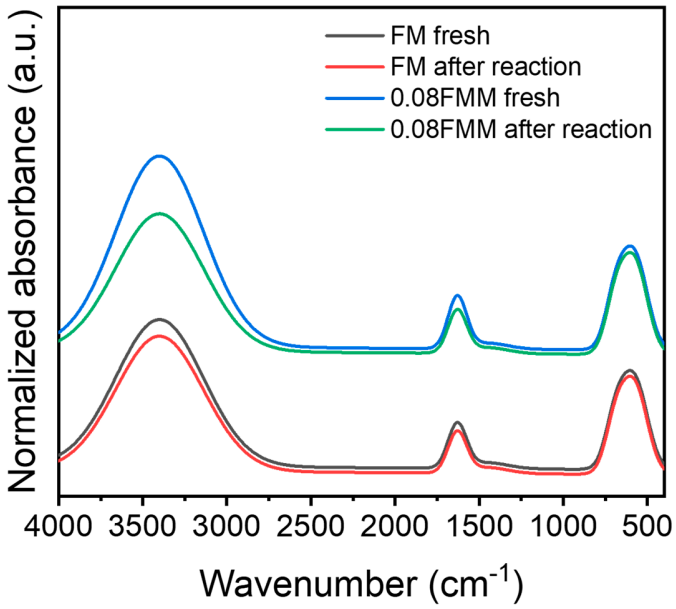


Fig. S6 ATR-FTIR spectra of FM and 0.08FMM before and after catalytic ozonation.

S7 EPR spin-trapping measurements

DMPO spin-trapping EPR measurements were used to directly probe radical formation in the ozonation systems. The comparison included O_3 alone, FM + O_3, 0.08FMM + O_3, and 0.08FMM + O_3 in the presence of TBA. DMPO was added immediately before ozone exposure, and spectra for all systems were collected under identical acquisition conditions immediately after treatment. The 0.08FMM + O_3 system exhibited the strongest characteristic four-line DMPO–OH signal with an approximate 1:2:2:1 intensity pattern; O_3 alone gave a weak signal and FM + O_3 an intermediate signal. With the integrated DMPO–OH signal of 0.08FMM + O_3 normalized to 1.00, the corresponding intensities were ~0.18 for O_3 alone, ~0.50 for FM + O_3, and ~0.21 for 0.08FMM + O_3 + TBA. The strong enhancement by 0.08FMM and suppression by TBA support HO· generation in the catalytic system. Measurements were conducted in X-band mode at room temperature, and identical instrumental settings were used for all samples.

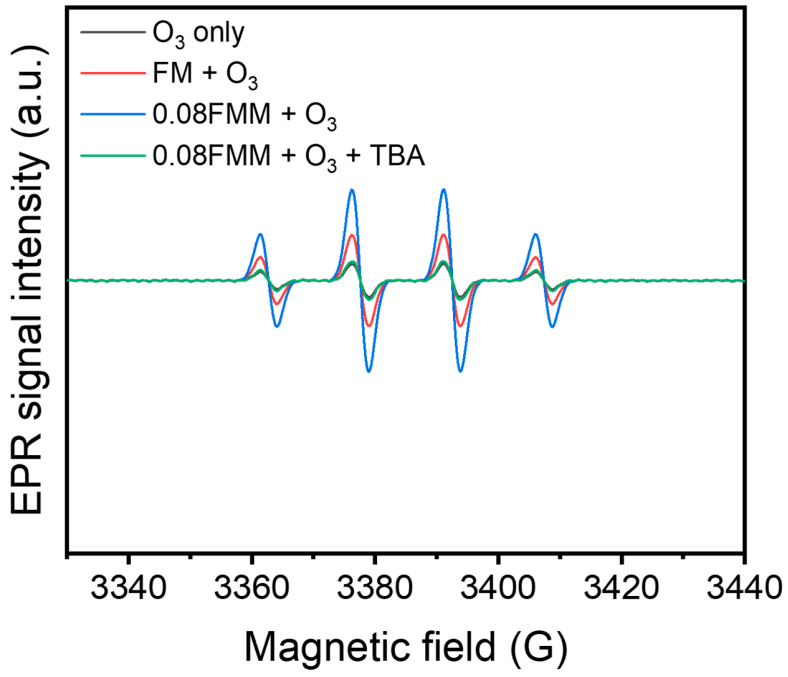


Fig. S7 DMPO spin-trapping EPR spectra of the O_3-only, FM + O_3, 0.08FMM + O_3, and 0.08FMM + O_3 + TBA systems.

S8 Mineralization under optimized conditions

Phenol removal and TOC removal were compared under the preliminary and optimized electrodeposition conditions to distinguish disappearance of the parent phenol compound from overall organic-carbon removal. Under the optimized condition (±180 mA, 9000 s), 0.08FMM achieved 87.8% phenol removal and 60.5% TOC removal after 30 min. The TOC removal increased from 51.4% under the preliminary condition to 60.5% after optimization, but remained substantially below the phenol-removal value, confirming that partially oxidized organic intermediates persisted after 30 min and that phenol disappearance should not be equated with complete mineralization.

Table S3 Phenol and TOC removal over 0.08FMM under preliminary and optimized electrodeposition conditions.

Condition	Electrodeposition condition	Phenol removal (%)	TOC removal (%)
Preliminary 0.08FMM	±240 mA, 9000 s	77.3	51.4
Optimized 0.08FMM	±180 mA, 9000 s	87.8	60.5

Catalytic test conditions: $[phenol]_0$ = 300 mg L^{-1}, O_3 feed rate = 6 mg min^{-1} (0.2 L min^{-1} pure O_2 carrying 30 mg L^{-1} O_3), catalyst loading ~1 g, 25 °C, and 30 min reaction time.

References

30. Kasprzyk-Hordern, B.; Ziółek, M.; Nawrocki, J. Catalytic ozonation and methods of enhancing molecular ozone reactions in water treatment. *Appl. Catal. B Environ.* **2003**, *46*, 639–669.
31. Wang, J.; Chen, H. Catalytic ozonation for water and wastewater treatment: Recent advances and perspective. *Sci. Total Environ.* **2020**, *704*, 135249.